Journal of Machine Construction and Maintenance
QUARTERLY 3/2019(114)
ISSN 1232-9312
p. 31–38

Jerzy SMOLIK[a,*], Adam MAZURKIEWICZ[a], Jan BUJAK[a], Daniel PAĆKO[a], Łukasz ROGAL[b]
[a] Łukasiewicz Research Network – Institute for Sustainable Technologies, Radom, Poland
[b] Institute of Metallurgy and Materials Science of Polish Academy of Sciences, Cracow, Poland
* Corresponding author: jerzy.smolik@itee.radom.pl

ANALYSIS OF FATIGUE STRENGTH OF MULTI-LAYER COATINGS TYPE Cr / CrN / (CrN-Me_1Me_2N)$_{multinano}$ / (Me_1Me_2N-VN)$_{multinano}$

Key words: multi-layer coatings, fatigue strength.

Abstract: The article presents the results of tests of resistance to mechanical fatigue of multilayer coatings type Cr / CrN / (CrN-Me1Me2N) $_{multinano}$ / (Me1Me2N-VN) $_{multinan}$, where metals Me1 and Me2 were chosen from Al, Cr, Ti, Zr, and Si. Multilayer coatings designed for the research were generated by the Arc Evaporation method. On the basis of the results of hardness and adhesion tests, calculations of the fatigue strength of the multilayer coatings were carried out. The obtained results showed that the chemical composition of individual component layers in the multilayer coating can be decisive in the process of creating a microstructure resistant to the fatigue cracking process.

Analiza wytrzymałości zmęczeniowej powłok wielowarstwowych typu Cr / CrN / (CrN-Me_1Me_2N)$_{multinano}$ / (Me_1Me_2N-VN)$_{multinano}$

Słowa kluczowe: powłoki wielowarstwowe, odporność zmęczeniowa.

Streszczenie: W artykule przedstawiono wyniki badań odporności na zmęczenie mechaniczne powłok wielowarstwowych typu Cr / CrN / (CrN-Me_1Me_2N)$_{multinano}$ / (Me_1Me_2N-VN)$_{multinano}$, gdzie metale Me_1,Me_2 dobierano spośród Al, Cr, Ti, Zr, Si. Powłoki wielowarstwowe przeznaczone do badań wytworzono metodą Arc Evaporation. Na podstawie wyników badań twardości i adhezji przeprowadzono obliczenia wytrzymałości zmęczeniowej badanych powłok wielowarstwowych. Badania wykazały, że skład chemiczny poszczególnych warstw składowych w powłoce wielowarstwowej może mieć decydujące znaczenie w procesie tworzenia się mikrostruktury odpornej na proces pękania zmęczeniowego.

Introduction

Better tribological properties of cooperating elements are usually achieved by increasing the hardness and reducing the coefficient of friction [1–3]. However, in modern production processes, both tools and machine components are exposed additionally to the action of high-speed mechanical loads, which are often also connected with cyclic temperature impact, such as in pressure die casting [4–5] or die forging hot [6–7]. Therefore, thinking about increasing the service life of machine elements and tools intended for high-speed, fast-changing production processes, it is necessary to ensure their high resistance to mechanical fatigue.

New material and technological development in the field of surface engineering, including the production of layers and coatings, enables modifying the properties of the surface layer of the elements of tools and machines, thanks to which, they can be better adapted to work in difficult and more demanding operating conditions. The multilayered coating creates very large possibilities in the area of shaping the properties of the surface layer. A characteristic feature of multilayer coatings is the ability to design properties as a function of their thickness, e.g., by changing the amount, thickness, and the order of component layers in multilayer coatings [8–9] and the correct selection of microstructure, chemical composition, and phase composition of individual component layers [10–11].

Interesting coating materials often used in the process of reducing the coefficient of friction are materials characterized by the presence of easy slip planes, including transition metal halides [12–14] that include MoS_2, WS_2, and $NbSe_2$, as well as hard metal oxide phases [15–17] that include WO_3, V_2O_5, and MoO_3. These phases, referred to as Magnelli oxide phases, are the oxidation products of the metallic components that make up the coating. Among the oxides mentioned above, the vanadium oxide phases V_2O_5 and $AlVO_4$ create a good chance to use as a lubricant. This is documented by anti-wear coatings with TiAlN/VN superstructure structure [18], and with multi-component coatings doped with vanadium (TiAlV)N [19] and (AlCrV)N [20], whose coefficient of friction at elevated temperatures (≈700°C) has been reduced to values of 0.2–0.3.

The article presents the results of tests of resistance to mechanical fatigue of multilayer coatings type Cr / CrN / (CrN-Me1Me2N) $_{multinano}$ / (*Me1Me2*N-VN) $_{multinan}$, where metals *Me1 and Me2* were chosen from Al, Cr, Ti, Zr, and Si.

1. Experimental procedure

1.1. Coating deposition

The coatings were obtained on a nitrided steel substrate ENX40CrMoV5.1. The proposed PVD coatings consist of three zones. Zone 1 is the Cr/CrN complex located directly on the tool surface, providing the required adhesion to the substrate. Zone 2 is a nano-multilayered coating (CrN-*Me1Me2*N) $_{multinano}$, which is the transition zone between the "adhesive complex" and Zone 3 and responsible for cooperation with the external material. Zone 3 is responsible for the reduction of the coefficient of friction, and it is alternating applied layers of *Me1Me2*N and VN, with nanometric thicknesses.

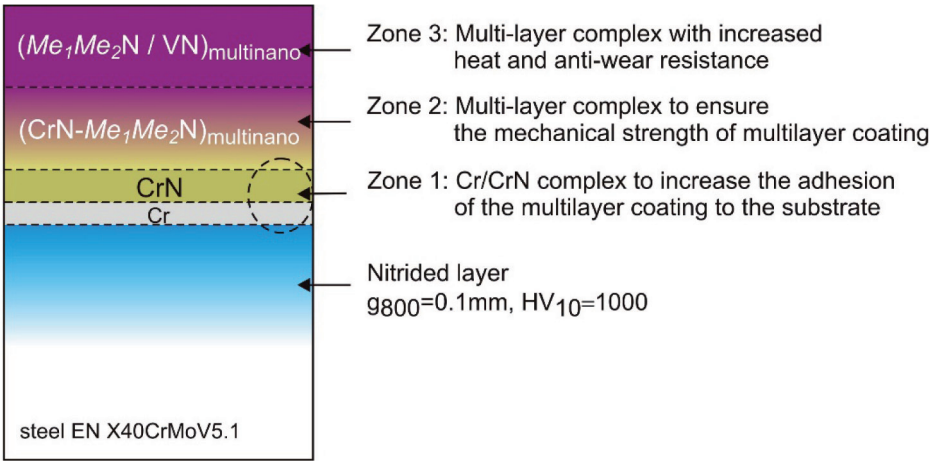

Fig. 1. Scheme of multilayer coatings selected for testing

On the basis of the analysis, 5 different multilayer coatings were prepared for the research on nitrided steel ENX40CrMoV5.1 (nitrided layer: HV10 = 1000–1100 HV, gHV800 ≈ 0.07 mm), according to the diagram shown in Figure 1, which are as follows:

Cr-CrN / (CrN-CrAlN)$_{multinano}$ / (CrAlN-VN)$_{multinano}$
Cr-CrN / (CrN-TiAlN)$_{multinano}$ / (TiAlN-VN)$_{multinano}$
Cr-CrN / (CrN-TiZrN)$_{multinano}$ / (TiZrN-VN)$_{multinano}$
Cr-CrN / (CrN-CrSiN)$_{multinano}$ / (CrSiN-VN)$_{multinano}$
Cr-CrN / (CrN-VN)$_{multinano}$

Multilayer coatings for testing were prepared by Arc Evaporation [21–22] using the MZ383 technology device from Metaplas Ionon. The composition of cathode arc sources and their location in the process chamber during coating deposition are shown in Fig. 2. Multilayer complexes (CrN-*Me1Me2*N) $_{multinano}$ and (*Me1Me2*N-VN) $_{multinan}$ have been obtained by introducing the rotation of the coated substrate around the axis of the process chamber, as seen in Fig. 2a. The rotational speed was 5 rpm, which means that alternating layers of constituents were produced within one minute, i.e. 5 layers of CrN and 5 layers of *Me1Me2*N.

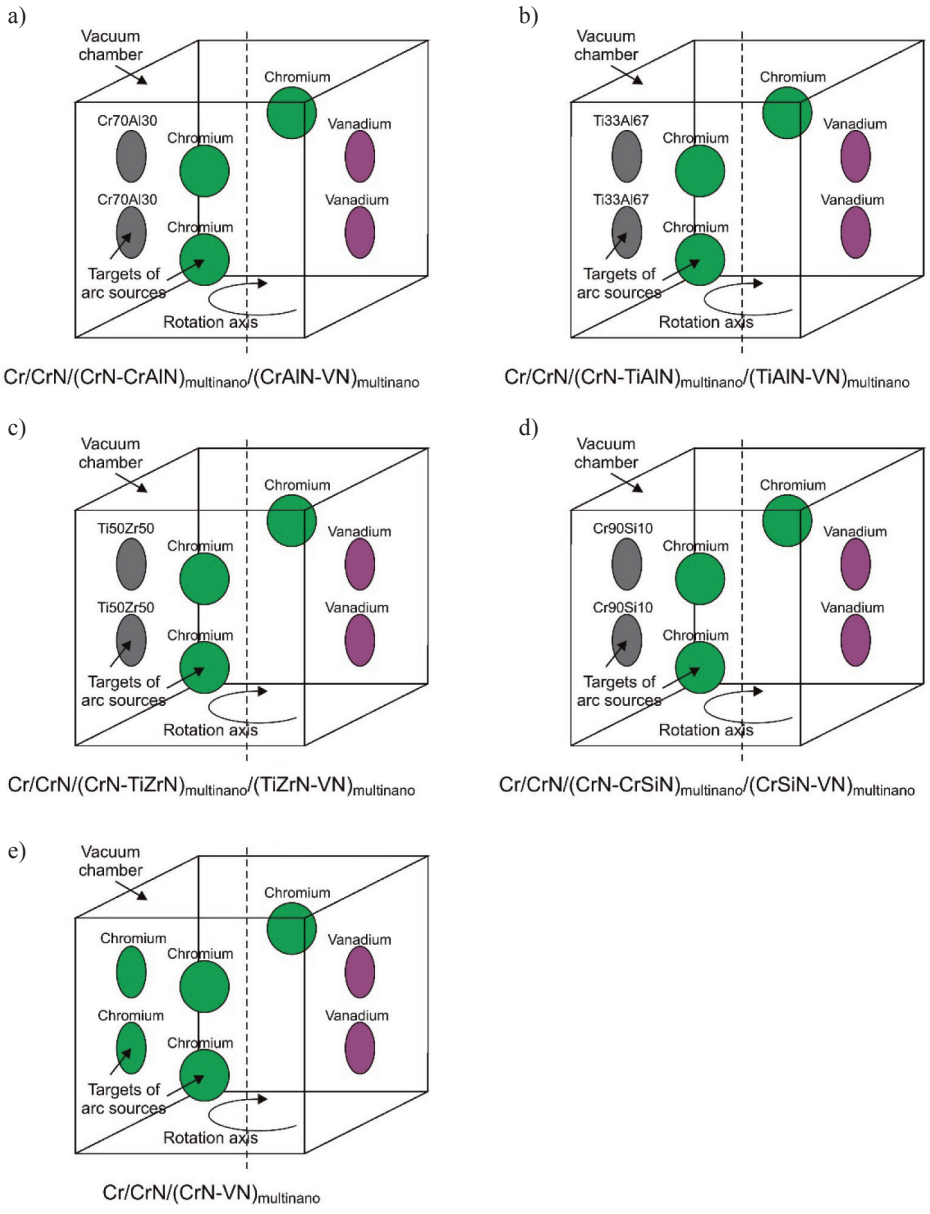

Fig. 2. The composition of cathodes and the location of arcing sources in the process chamber, in the manufacturing processes of selected multilayer coatings

1.2. Coating characterization

The conducted literature analysis in the field of testing the resistance of thin coatings to mechanical fatigue [23–24] has shown that it is possible to use the procedure proposed by Hikmet Cicek, et al. [25]. According to the proposed procedure, the fatigue properties of a coating are significantly influenced by the following properties: the ratio of the substrate hardness and coating (H_s/H_f), the thickness of the coating (g), and the critical load that generates a coating loss of adhesion (F_c). Analysis of the presented correlations made it possible to develop the following empirical formula (Equation 1) defining the relationship between fatigue strength of coatings and its material properties:

$$W_z = \frac{H_s}{H_f} \cdot F_c \cdot g \ [\mathrm{N} \cdot \mu\mathrm{m}] \tag{1}$$

where

W_z – fatigue strength,
H_f – hardness of coating [GPa],
H_s – hardness of substrate [GPa],
F_c – adhesion of coating [N],
g – thickness of coating [μm].

The hardness of the tested multilayer coatings (H_f) was determined using NHT nano-spheres and a Berkovich indenter. In order to eliminate the influence

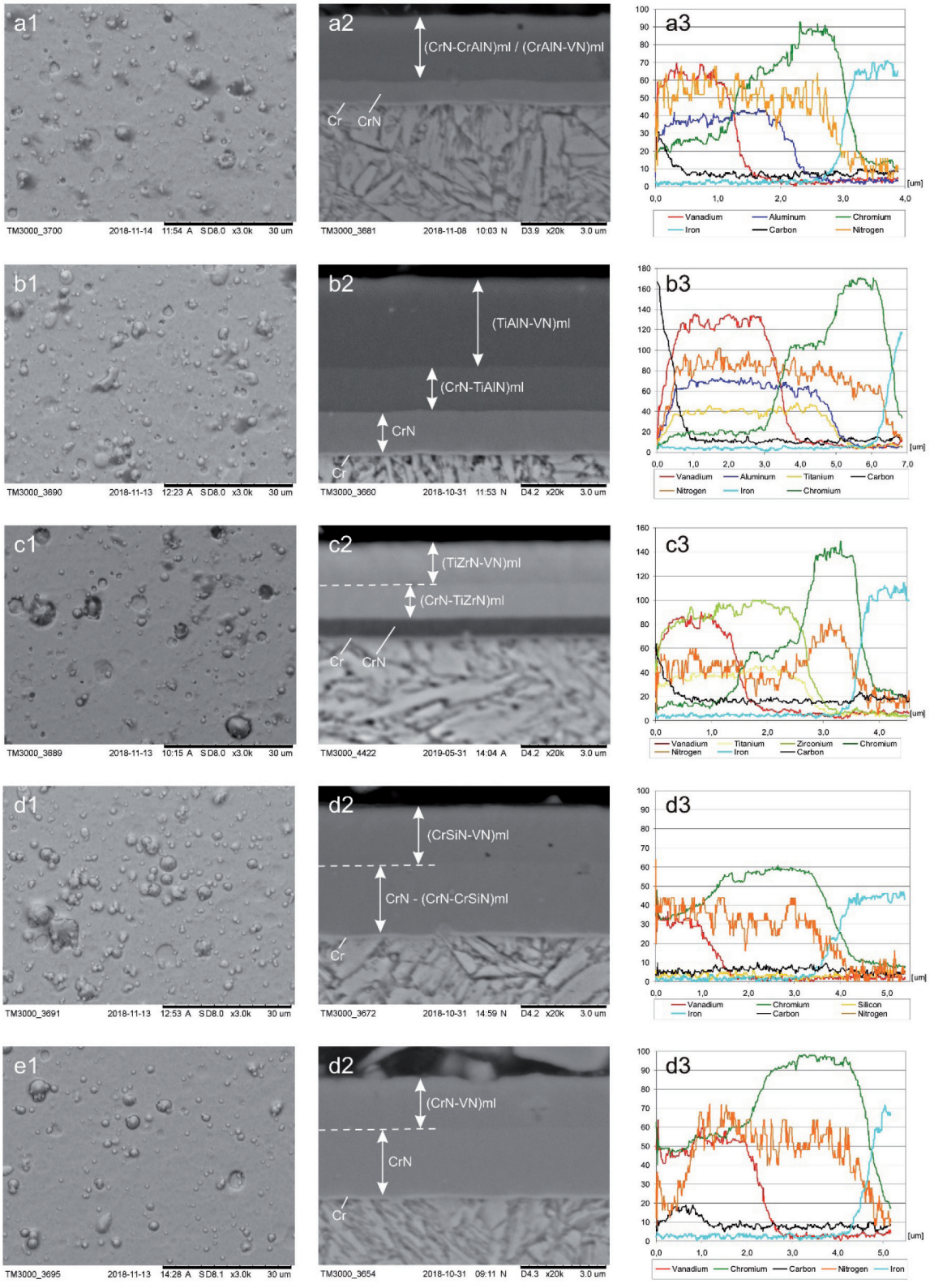

Fig. 3. Characteristics of the tested multilayer coatings: 1 – surface topography, 2 – cross section, 3 – linear analysis of chemical composition as a function of distance from the surface; a – Cr-CrN / $(CrN\text{-}CrAlN)_{multinano}$ / $(CrAlN\text{-}VN)_{multinano}$, b – Cr-CrN / $(CrN\text{-}TiAlN)_{multinano}$ / $(TiAlN\text{-}VN)_{multinano}$, c – Cr-CrN / $(CrN\text{-}TiZrN)_{multinano}$ / $(TiZrN\text{-}VN)_{multinano}$, d – Cr-CrN / $(Cr\ N\text{-}CrSiN)_{multinano}$ / $(CrSiN\text{-}VN)_{multinano}$, e – Cr-CrN / $(CrN\text{-}VN)_{multinano}$

of substrate parameters on the measurement results, the tests were carried out in the mode of a limited indentation to a depth of h <300 nm, where h <10% of the coating thickness. For each coating, 10 representative hardness measurements were made, and then mean values were determined.

The value of critical adhesion force (Fc2) was determined by the scratch-test method, using REVETEST CSM and a Rockwell type penetrator. Scratches were made in the linear increase mode of the penetrator load in the range of 0–200 N and the rate of load increase ΔF = 10 N/mm. The values of the critical adhesion force Fc2, which is the inductor load at which loss of adhesion of the coating to the substrate occurs, was determined on the basis of the analysis of changes in coefficient of friction, the emission level of acoustic signal AE, and scratches on the basis of microscopic observations.

The analysis of surface topography, observations of cross-sections, as well as thickness analysis of multilayer coatings were made using Scanning Electron Microscopy – SEM (Hitechi TM3000).

In order to verify the structure of multilayer PVD coatings, analysis of changes in chemical composition as a function of distance from the surface was made by EDS – Energy Dispersive X-ray Spectroscopy.

2. Results and discussion

2.1. Microscopic observation and analysis of chemical composition

The results of microscopic analysis of surface topography, the multilayer structure, and the linear changes in chemical composition as a function of distance from the surface of the multilayer coatings tested are shown in Fig. 3. All coatings produced, regardless of chemical composition, have similar surface roughness values in the range: Ra = 0.14–0.20 μm, Rz = 1.36––2.02 μm, and Rt = 2.19–2.62 μm. On the surface of coatings (a1 to a5), micro-sprinkles of targets are visible, which is a characteristic feature of PVD coatings produced by the Arc Evaporation method.

Microscopic observations of cross sections (b1 – b5) and the results of a linear analysis of changes in the chemical composition (c1 – c5) confirmed that the multilayer structure of the tested coatings is consistent with the design shown in Fig. 1.

2.2. Hardness measurements

Hardness and Young's modulus measurements indicated that the developed multilayer coatings have hardness values in the range H ≈ 21.8–25.6 GPa and Young's modulus values in the range E ≈ 327–440 GPa. All measurements were made at the same depth of penetration of h = 300 nm. The force acting on the indenter varied depending on the hardness of the coating in the range of 41–51 mN. The diversified hardness and Young's modulus values influence the elastic-plastic properties of the tested coatings, including resistance to elastic deformation (H / E) and resistance to plastic deformation (H^3/E^2). The results of the hardness and Young's modulus measurements carried out and the determined H/E and H^3/E^2 indices are shown in Table 1.

Table 1. The results of hardness and Young's modulus measurements

Multilayer coating	Hardness of coating H [GPa]	Young Modulus E [GPa]	Resistance to elastic deformation H/E	Resistance to plastic deformation H^3/E^2
Cr-CrN / $(CrN\text{-}CrAlN)_{multinano}$ / $(CrAlN\text{-}VN)_{multinano}$	25.4 ± 1.2	373 ± 28	0.068	0.117
Cr-CrN / $(CrN\text{-}TiAlN)_{multinano}$ / $(TiAlN\text{-}VN)_{multinano}$	25.6 ± 1.4	400 ± 37	0.064	0.105
Cr-CrN / $(CrN\text{-}TiZrN)_{multinano}$ / $(TiZrN\text{-}VN)_{multinano}$	24.9 ± 1.7	353 ± 16	0.071	0.124
Cr-CrN / $(CrN\text{-}CrSiN)_{multinano}$ / $(CrSiN\text{-}VN)_{multinano}$	23.2 ± 1.5	333 ± 20	0.070	0.113
Cr-CrN / $(CrN\text{-}VN)_{multinano}$	21.8 ± 1.6	327 ± 21	0.067	0.097

2.3. Adhesion measurements

On the basis of microscopic observations of scratches, it was found that, as a result of elastic and plastic deformations of the coating, forced by the increasing load of the penetrator, a characteristic multi-step failure mechanism in the scratch test was revealed in all of the tested coatings. In the first phase, i.e. in the load range of 42–65 N, the cracking of the tested coatings occurs – cohesive damage (Fc1). With a further increase in the load acting on the indenter, in the range

of 65–133 N, the process of adhesion damage (Fc2) generation starts, i.e. the coating defects mainly on the scratch edges. After exceeding the load value of 150 N, the most intensive mechanism of destroying the coatings is abrasive wear, which leads to the complete removal of the coating from the surface of the steel substrate (Fc3). Adhesion test results are shown in Table 2.

Table 2. The results of adhesion measurement with use the scratch-test method

Multilayer coating	Fc1 [N] indenter load causing cohesive damage of the coating	Fc2 [N] indenter load causing adhesive damage of the coating	Fc3 [N] load of the indenter causing complete removal of the coating from the surface of the substrate
Cr-CrN / $(CrN\text{-}CrAlN)_{multinano}$ / $(CrAlN\text{-}VN)_{multinano}$	56	133	176
Cr-CrN / $(CrN\text{-}TiAlN)_{multinano}$ / $(TiAlN\text{-}VN)_{multinano}$	64	95	160
Cr-CrN / $(CrN\text{-}TiZrN)_{multinano}$ / $(TiZrN\text{-}VN)_{multinano}$	42	63	156
Cr-CrN / $(CrN\text{-}CrSiN)_{multinano}$ / $(CrSiN\text{-}VN)_{multinano}$	48	113	180
Cr-CrN / $(CrN\text{-}VN)_{multinano}$	44	130	151

2.4. Fatigue strength analysis

On the basis of the results of the hardness tests (Table 1) and adhesion (Table 2), fatigue strength calculations of the tested multilayer coatings were carried out according to Equation 1. The results of calculations are shown in Table 3.

Table 3. The results of strength fatigue of multilayer coating calculation

Multilayer coating	Hs [GPa]	H [GPa]	Adhesion Fc2 [N]	Thickness of coating [μm]	Strength fatigue Wz [Nμm]
Cr-CrN / $(CrN\text{-}CrAlN)_{multinano}$ / $(CrAlN\text{-}VN)_{multinano}$	11	25.4	133	3.5	201
Cr-CrN / $(CrN\text{-}TiAlN)_{multinano}$ / $(TiAlN\text{-}VN)_{multinano}$	11	25.6	95	3.4	139
Cr-CrN / $(CrN\text{-}TiZrN)_{multinano}$ / $(TiZrN\text{-}VN)_{multinano}$	11	24.9	63	3.7	103
Cr-CrN / $(CrN\text{-}CrSiN)_{multinano}$ / $(CrSiN\text{-}VN)_{multinano}$	11	23.2	113	3.1	165
Cr-CrN / $(CrN\text{-}VN)_{multinano}$	11	21.8	130	3.7	240

The calculations indicated that the greatest fatigue strength is characterized by the multilayer coating Cr-CrN / $(CrN\text{-}VN)_{multinano}$. Of all the multilayer coatings tested, the Cr-CrN / (CrN-VN) coating is characterized by the highest content of the chromium nitride phase – CrN. The presence of the CrN phase increases the plasticity of the coating, and it results in increases of the adhesion of the Fc2 coating and simultaneously stabilizes its hardness at 20–22 GPa. As a result, the fatigue strength of coatings with high CrN content is usually high.

At the same time, the calculations indicated that the multi-layer coating Cr-CrN / $(CrN\text{-}CrAlN)_{multinano}$ / $(CrAlN\text{-}VN)_{multinano}$, despite much greater hardness and lower thickness, it is also characterized by a high fatigue strength of more than 200 [N·μm].

Conclusions

On the basis of the material test results, it should be assumed that the most promising material solution for applications exposed to complex destructive factors, i.e. intensive abrasive wear combined with cyclically changing mechanical loads, is the Cr – CrN / (CrN – CrAlN) $_{multinano}$ coating / (CrAlN - VN) $_{multinano}$.

It is characterized by high hardness (H = 25.4 GPa) and high Young's modulus (E = 373 GPa), which ensures its resistance to plastic deformation (H3/E2 = = 0.117). Due to the high hardness, one should also expect a high abrasion resistance. At the same time, this coating is characterized by high fatigue strength at the level of Wz = 201 [N·μm], which ensures its durability in applications with cyclically variable external loads.

The conducted research has shown that the chemical composition of individual component layers can be decisive in the process of creating a microstructure resistant to the fatigue cracking process.

Acknowledgements

Work executed within the project entitled "Creation of the Intelligent Specialisation Centre in the Field of Innovative Industrial Technologies and Technical and Environmental Safety" is financed from the Regional Operational Programme of the Mazowieckie Voivodeship 2014–2020.

References

1. Hogmmark S., Jacobson S., Larsson M.: Design and evaluation of tribological coatings. *Wear*, 2000, 246, pp. 20–33.
2. Bobzin K.: High-performance coating for cutting tools. *CIRP Journal of Manufacturing Science and Technology*, 2017, 18, pp. 1–9.
3. Hong D., Niu Y., Li H., Zhong X., Sun J.: Comparison of microstructure and tribological properties of plasma-sprayed TiN, TiC and TiB_2 coatings. *Surface and Coatings Technology*, 2019, 374, pp. 181–188.
4. Hovsepian P.Eh., Luo Q., Robinson G., Pittman M., Howarth M., Doerwald D., Tietema R., Sim W.M., Deeming A., Zeus T.: TiAlN/VN superlattice structured PVD coatings: A new alternative in machining of aluminium alloys for aerospace and automotive components. *Surface and Coatings Technology*, 2006, 201(1–2), pp. 265–272.
5. Ilyuschenko A.Ph., Feldshtein E.E., Lisovskaya Y.O., Markova L.V., Andreyev M.A., Lewandowski A.: On the properties of PVD coating based on nanodiamond and molybdenum disulfide nanolayers and its efficiency when drilling of aluminum alloy. *Surface and Coatings Technology*, 2015, 270, pp. 190–196.
6. Smolik J., Walkowicz J., Tacikowski J.: Influence of the structure of the composite: "nitrided layer / PVD coating" on the durability of tools for hot-working. *Surface and Coatings Technology*, 2000, 125, pp. 134–140.
7. Persson A., Hogmark S., Bergström J.: Thermal fatigue cracking of surface engineered hot work tool steel. *Surface and Coatings Technology*, 2005, 191, pp. 216–227.
8. Xu X., Su F., Li Z.: Tribological properties of nanostructured TiAlN/W_2N multilayer coating produced by PVD. *Wear*, 2019, 430–431, pp. 67–75.
9. Li Y., Ye Q., Zhu Y., Zhang L., He Y., Zhang S., Xiu J.: Microstructure, adhesion and tribological properties of CrN/CrTiAlSiN/WCrTiAlN multilayer coatings deposited on nitrocarburized AISI 4140 steel. *Surface and Coatings Technology*, 2019, 362, pp. 27–34.
10. Kim Y.J., Byun T.J., Han J.G.: Bilayer period dependence of CrN/CrAlN nanoscale multilayer thin films. *Superlattices and Microstructures*, 2009, 45(2), pp. 73–79.
11. Smolik J., Zdunek K., Larisch B.: Investigation of adhesion between component layers of a multi-layer coating TiC/Ti(C_xN_{1-x})/TiN by the scratch test method. *Vacuum*, 1999, 55(1), pp. 45–50.
12. Kim S.K., Ahn Y.H., Kim K.H.: MoS_2-Ti composite coatings on tool steel by d.c. magnetron sputtering. *Surface and Coatings Technology*, 2003, 169–170, pp. 428–432.
13. Renevier N.M., Fox V.C., Teer D.G., Hampshire J.: Coating characteristics and tribological properties of sputter-deposited MoS_2/metal composite coatings deposited by closed field unbalanced magnetron sputter ion plating. *Surface and Coatings Technology*, 2000, 127(1), pp. 24–37.
14. Carmalt C.J., Manning T.D., Parkin I.P., Peters E.S., Hector A.L.: NbS_2 thin films by atmospheric pressure chemical vapour deposition and the formation of a new 1T polytype. *Thin Solid Films*, 2004, 469–470, pp. 495–499.
15. Lewis D.B., Creasey S., Zhou Z., Forsyth J.J., Ehiasarian A.P., Hovsepian P.Eh., Luo Q., Rainforth W.M., Münz W.-D.: The effect of (Ti+Al):V ratio on the structure and oxidation behaviour of TiAlN/VN nano-scale multilayer coatings. *Surface and Coating Technology*, 2004, 177–178, pp. 252–259.
16. Arenas M.A., Ahuir-Torres J.I., García I., Carvajal H., de Damborenea J.: Tribological behaviour of laser textured Ti6Al4V alloy coated with MoS_2 and graphene. *Tribology International*, 2018, 128, pp. 240–247.

17. Daniyan A.A., Umoru L.E., Popoola A.P.I., Fayomi O.S.I.: Comparative studies of microstructural, tribological and corrosion properties of Zn-TiO_2 and Zn-TiO_2-WO_3 nano-composite coatings. *Results in Physics*, 2017, 7, pp. 3222–3229.
18. Mayrhofer P.H., Hovsepian P.Eh., Mitterer C., Münz W.-D.: Calorimetric evidence for frictional self-adaptation of TiAlN/VN superlattice coatings. *Surface and Coatings Technology*, 2004, 177–178, pp. 341–347.
19. Kutschej K., Mayrhofer P.H., Kathrein M., Polcik P., Mitterer C.: A new low-friction concept for $Ti_{1-x}Al_xN$ based coatings in high-temperature applications. *Surface and Coatings Technology*, 2004, 188–189, pp. 358–363.
20. Franz R., Neidhardt J., Sartory B., Kaindl R., Tessadri R., Polcik P., Derflinger V.H.: High-temperature low-friction properties of vanadium-alloyed AlCrN coatings. *Tribology Letters*, 2006, 23, pp. 101–107.
21. Raab R., Koller C.M., Kolozsvári S., Ramm J., Mayrhofer P.H.: Thermal stability of arc evaporated Al-Cr-O and Al-Cr-O/Al-Cr-N multilayer coatings. *Surface and Coatings Technology*, 2018, 25, pp. 213–221.
22. Zhu L-H., Song Ch., Ni W-Y., Liu Y-X.: Effect of 10% Si addition on cathodic arc evaporated TiAlSiN coatings. *Transactions of Nonferrous Metals Society of China*, 2016, 26(6), pp. 1638–1646.
23. Yildiz F., Alsaran A.: Multi-pass scratch test behavior of modified layer formed during plasma nitriding. *Tribology International*, 2010, 43, pp. 1472–1478.
24. Arslan E., Baran Ö., Efeoglu I., Totik Y.: Evaluation of adhesion and fatigue of MoS_2–Nb solid-lubricant films deposited by pulsed-dc magnetron sputtering. *Surface and Coatings Technology*, 2008, 202, pp. 2344–2348.
25. Cicek H., Baran O., Keles A., Totik Y., Efeoglu I.: A comparative study of fatigue properties of TiVN and TiNbN thin films deposited on different substrates. *Surface and Coatings Technology*, 2017, 332, pp. 296–303.